



Mass unloading along the inner edge of the Enceladus plasma torus

W. M. Farrell,¹ M. L. Kaiser,¹ D. A. Gurnett,² W. S. Kurth,² A. M. Persoon,²
J. E. Wahlund,³ and P. Canu⁴

Received 12 October 2007; revised 12 November 2007; accepted 29 November 2007; published 23 January 2008.

[1] A major discovery made by the Cassini spacecraft at Saturn was the substantial mass ejection from the south pole of Enceladus. Previous studies show that this ejected gas can become ionized and subsequently load mass onto the connecting magnetic field lines near the moon. Radial diffusion then allows the mass-loaded field lines to move outward to $\sim 15 R_s$ and inward to $\sim 2 R_s$, forming a plasma torus. We demonstrate herein that the mass is also “unloaded” along the inner edge of this plasma torus - the edge incident with the plasma-absorbing A-ring. Interpreting down-drifting z-mode tones from active sites along the inner edge of the ion torus as emission near the local electron plasma frequency, f_{pe} , we can remotely monitor this reduction in plasma density along the torus inner edge as a function time. We find that the down-drift of the z-mode tones corresponds typically to a plasma density change $dn/dt \sim -5 \times 10^{-4}/\text{cm}^3\text{-s}$ and when integrated over an annulus defined by the outer edge of the A-ring, corresponds to a mass loss of ~ 40 kg/s. Using the z-mode tones, we also find locations where plasma mass from the ring-ionosphere is possibly loaded at 1–2 kg/s onto field lines near the Cassini gap. **Citation:** Farrell, W. M., M. L. Kaiser, D. A. Gurnett, W. S. Kurth, A. M. Persoon, J. E. Wahlund, and P. Canu (2008), Mass unloading along the inner edge of the Enceladus plasma torus, *Geophys. Res. Lett.*, *35*, L02203, doi:10.1029/2007GL032306.

1. Introduction

[2] Hubble Space Telescope (HST) UV observations [Shemansky *et al.*, 1993; Richardson *et al.*, 1998; Jurac *et al.*, 2002] indicated the surprising presence of a large concentration of hydroxyl radicals indicative of neutral water molecules located near 4 Saturn radii from the planet. At the time, the source was not uniquely identified. Subsequent Cassini imaging observations have directly revealed the source as active water geysers from the south pole of the moon Enceladus [Porco *et al.*, 2006; Waite *et al.*, 2006; Hansen *et al.*, 2006]. Models [Richardson and Jurac, 2004; Jurac and Richardson, 2005] suggest that charge exchange, photoionization, and electron impact ionization convert a substantial portion of the neutral component to a plasma that consequently gets picked up by Saturn’s magnetic field to

(approximately) corotate with the planet. The newly-created plasma radially diffuses both inward and outward to then form a substantial plasma torus that extends from $\sim 2 R_s$ to $\sim 15 R_s$ [see Richardson and Jurac, 2004, Figure 1]. This diffusion is associated with violation of the third adiabatic invariant, with an assumed model diffusion coefficient that varies as $1/r^3$ [Richardson and Jurac, 2004]. Johnson *et al.* [2006] recently demonstrated that that charge exchange and neutral scattering also give rise to substantial cross-field migration of Enceladus plasma and neutrals. In situ observations of electron density from the Cassini Radio and Plasma Wave (RPWS) instrument [Gurnett *et al.*, 2004; Wahlund *et al.*, 2005] clearly confirm the presence of this torus having peak electron densities of $150/\text{cm}^3$ near $3 R_s$ [Gurnett *et al.*, 2005] and an electron density profile that varies as $1/r^4$ in the torus outer region beyond $5 R_s$ [Persoon *et al.*, 2005, 2006]. In this work, we focus on the detailed structure of the torus’ inner edge, where the plasma encounters the relatively-thick A ring.

[3] Examining the changes in convected plasma flow in the vicinity of Enceladus, Tokar *et al.* [2006] and Pontius and Hill [2006] found that the emitted gasses are ionized and mass loaded onto passing magnetic field lines at a rate of 100–200 kg/s. Gurnett *et al.* [2007] recently demonstrated that the plasma density and B-field in the plasma torus are phased with the auroral current system that generates Saturn Kilometric Radiation (SKR). They thus conclude that any Enceladus-related mass loading that slows the magnetic field lines relative to corotation must also then slow the magnetically-connected SKR radio source location, thereby creating secular variations in the measured radio rotation period.

[4] Richardson and Jurac [2004] presented a detailed transport model of the ion torus assuming a gas source of $\sim 10^{28}$ H_2O molecules/s near the orbit of Enceladus. They found that equatorial electron densities had peak values exceeding $100/\text{cm}^3$ between 3–4 R_s and that water and hydroxyl ion components each had peak values at $> 30/\text{cm}^3$ in the same region. Radial diffusion was included in the model, and the resulting torus was found to extend outward to $> 10 R_s$, appearing very similar to Cassini observations [see Persoon *et al.*, 2006, Figure 5]. The plasma torus was also found to diffuse inward to $< 2 R_s$.

[5] Plasma sources from other moons have been identified [Wahlund *et al.*, 2005] and they also contribute to this torus (also called by the generic name of the “plasma disk”). For this work, we focus on the Enceladus contribution, and thus refer to this disk as the “Enceladus plasma torus”. However, the names can be used interchangeably.

[6] The Richardson and Jurac model assumed that the rings perfectly absorb the incident plasma at 1.5 R_s , thereby creating a “hard” boundary at the torus inner edge. As a consequence, a very large plasma density gradient develops

¹NASA/Goddard Space Flight Center, Greenbelt, Maryland, USA.

²Department of Physics and Astronomy, University of Iowa, Iowa City, Iowa, USA.

³Swedish Institute of Space Physics, Uppsala, Sweden.

⁴Centre d’Etude des Environnements Terrestre et Planétaires, Velizy, France.

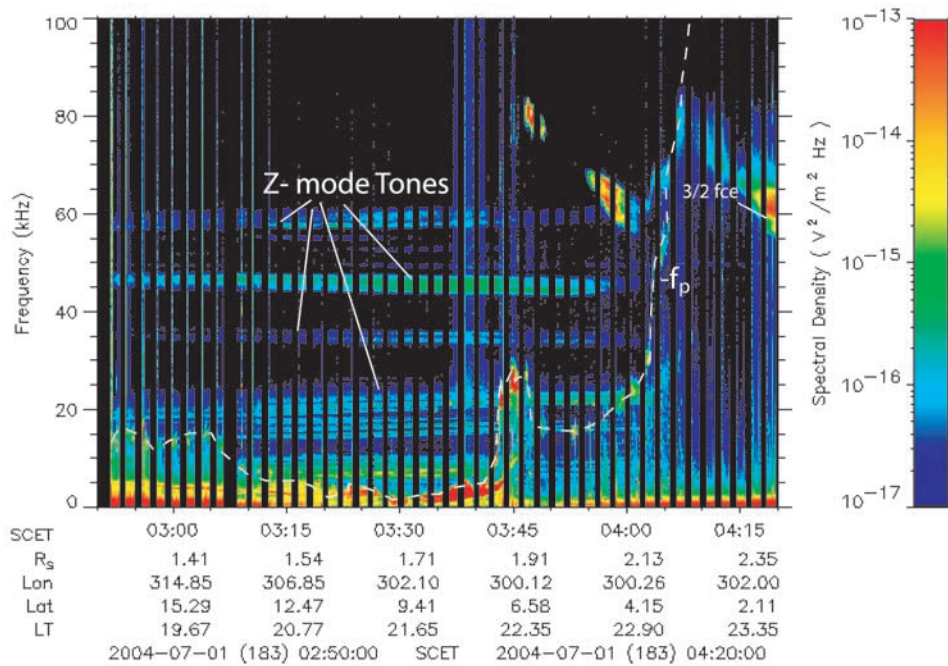


Figure 1. A Cassini RPWS radio spectrogram during Saturn Orbit Insertion that shows the propagation of z-mode tones in the low density region located just inside the Enceladus plasma torus.

in the model from peak electron density values of $100/\text{cm}^3$ at $3 R_s$ to zero at $1.5 R_s$. Cassini RPWS observations confirm the presence of this very sharp gradient with an observed electron density decrease of nearly 4 orders of magnitude between 2.2 and $1.7 R_s$ ($\sim 1/2$ a planetary radii [see Gurnett *et al.*, 2005, Figure 5; Wahlund *et al.*, 2005, Figure 1]), providing strong observational support for the model's ring absorption boundary. The outer edge of the A-ring was previously identified as a dominant absorber of high-energy particles [Van Allen *et al.*, 1980].

[7] It is thus clear that the high-quality plasma transport models of the inner torus [Jurac and Richardson, 2005] correspond nicely to RPWS electron density observations at the large-scale. However, RPWS observations reveal finer details about the inner torus edge that are quite worthy of comment herein. We demonstrate that the boundary condition at the rings is apparently “soft”, with the loss of torus plasma competing with a source of ring-ionospheric plasma. We also show that torus mass is indeed unloaded from field lines at the rings, and derive a rate of mass unloading based upon direct observations of this plasma loss.

2. Direct Observations of the Mass Unloading Process

[8] Figure 1 shows a Cassini RPWS wideband waveform frequency versus time spectrogram of wave activity during part of the orbit insertion period on 1 July 2004. During this time, Cassini was making a very close encounter over the top (north face) of the rings, passing as close as $1.41 R_s$ in radial distance to the planet and $\sim 0.2 R_s$ over the A ring. In reference to Figure 1, between 03:15 and 04:15 SCET, Cassini was passing over the nightside faces of the B and A rings. We note that between 03:00 and 03:43 SCET, the

electron plasma frequency is identified by the upper cutoff of an auroral hiss/whistler mode emission [Gurnett *et al.*, 2005; Xin *et al.*, 2006] while thereafter an obvious emission at the electron plasma frequency, f_{pe} , can be uniquely identified, this appearing as a steeply up-drifting narrow-band tone that is labeled as “ f_p ” on the figure [Gurnett *et al.*, 2005; Farrell *et al.*, 2005]. The electron density derived from this f_{pe} emission is consistent with independent RPWS/Langmuir Probe measurements [Wahlund *et al.*, 2005]. The electron density in the inner magnetosphere is thus easily derivable from RPWS via both natural emissions and probe measurements. This density is shown by Gurnett *et al.* [2005, Figure 5] and Wahlund *et al.* [2005, Figure 1]. Between about 01:10 and 04:05 SCET, the electron plasma frequency is much less than the electron cyclotron frequency, $f_{pe} \ll f_{ce}$.

[9] The plasma morphology associated with Figure 1 is the following: Prior to about 03:45 SCET, Cassini was passing over the B ring and a low density plasma ($< 1 \text{ el}/\text{cm}^3$) was detected as indicated by the local plasma frequency below 10 kHz. Near 03:45, the plasma frequency had a localized maximum up to about 25 kHz ($\sim 8 \text{ el}/\text{cm}^3$), this in association with the passage of the spacecraft over the Cassini gap. After about 04:00 SCET, the spacecraft was passing into the inner edge of the Enceladus plasma torus, as identified by the quickly-increasing plasma frequency associated with the steep density gradient along this inner edge. As mentioned previously, the model of Jurac and Richardson [2004] also predicts the presence of this steep gradient along the radial inner edge, where the electron density changes by nearly 4 orders of magnitude between 03:30 and 04:10 SCET. Peak plasma frequencies associated with the torus are observed a short time later by Cassini

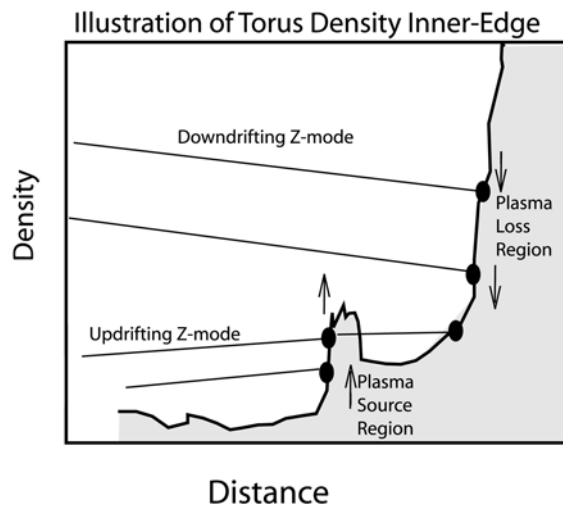


Figure 2. An illustration of the z-mode drift that is associated with changes at the radiation source. As density decreases along the inner edge of the Enceladus plasma torus, the z-mode tones (tied to the local plasma frequency) will subsequently downdrift with time. In contrast, a plasma source near the Cassini gap has a density increase as a function of time, giving rise to steadily updrifting tones.

RPWS with f_p extending above 100 kHz (densities exceeding $120 \text{ electron/cm}^3$) [Gurnett et al., 2005; Wahlund et al., 2005].

[10] Besides emissions at the plasma frequency, there is the presence of narrowband drifting tones in the spectrogram. A previous study [Farrell et al., 2005] identified these as remotely-propagating z-mode emissions which are found to easily penetrate into regions where $f < f_p$. The detailed arguments for z-mode emission are presented therein. The tones were found to be generated from locations having local intensifications and fluctuations of the f_p emission. It was analytically demonstrated that z-mode emission could be generated from such regions via wave conversion of the electrostatic whistler mode emissions near f_p to the z-mode at frequencies near $0.8 f_p$. Hence, these z-mode tones emitted from active regions allow investigators to remotely sense the plasma frequency (i.e., density) of the active sites along the inner torus edge for nearly an hour before the actual spacecraft interception through the edge. In essence, the tones “tag” active plasma sources at various locations, thereby allow a monitoring of source density temporal evolution along the inner edge of the torus.

[11] While the overall structure of the torus inner edge is in time-stationary equilibrium with the ring absorber, individual fluid elements diffuse inward and are absorbed at the rings. Hence, individual z-mode tones (radiating near f_{pe}) are assumed herein to be indicative of the plasma density associated with their respective source, which presumably evolves as the fluid evolves (decrease in density as the fluid diffuses inward). While this assumption is not unique, we will later present a strong validating argument.

[12] It was previously noted that narrow z-mode tones tended to form in sets (appearing as “bundles of straw” on a spectrogram) that shared a common drift in frequency

[Farrell et al., 2005]. Examining Figure 1, it is apparent that the tones above 30 kHz (like the very strong tone 45 kHz) tend to drift downward in frequency with time at a rate of about -3 kHz/hour , while the bundle of tones between 10 and 25 kHz tend to drift upward in time at a rate of $+4 \text{ kHz/hour}$ [Farrell et al., 2005]. If these drifts are related to changes in source plasma frequency, then the down-drifting tones at higher frequencies (those tones originating from the inner edge of the torus) are indicative of the plasma loss process - $dn/dt < 0$ (or $df_p/dt < 0$) - that is continuously operating to form the steep gradient along the inner Enceladus torus. Figure 2 illustrates the situation.

[13] In contrast, at lower frequencies (10–25 kHz) it is noted that these tones (originating from the local f_{pe} maximum at the Cassini gap) are primarily up-drifting, suggesting that there is a plasma source creating $dn/dt > 0$ (or $df_p/dt > 0$). Bouhram et al. [2006] presented a model of the ring ionosphere formed by radiation-induced decomposition of ice into free O_2 and demonstrated that the local plasma density increase centered at 03:45 SCET in Figure 1 originates from a ring-ionosphere plasma enhancement at the Cassini gap [see Bouhram et al., Figure 3]. Hence, this gap plasma is most likely not related to the Enceladus torus, but formed by field-aligned transport of plasma through the gap from the heavily-ionized southern side of the rings. The up-drifting z-mode tones provide observational support for an active source at the gap where plasma build up, $dn/dt > 0$, is ongoing.

[14] Because of this ring ionosphere, a “hard” inner torus boundary condition at the ring interface like that modeled by Richardson and Jurac [2004] is never really achieved: The electron density never actually drops to zero. The merger of torus plasma and ring plasma appears seamless - there is no discontinuity in plasma density (or f_p) where they merge (near 03:52 SCET in Figure 1). Only the z-mode emission, which records the change in f_p as a function of time, gives any indication of the likely plasma source.

[15] Table 1 lists the change in electron density as a function of time as derived from the drifting of specific brighter z-mode tones. This calculation assumes that the z-mode radiation is tied directly to the local plasma frequency of the active region where emission originates. Hence the drift in frequency represents the time-evolution of the electron density at the active site. We note that for emissions corresponding to the high-density inner torus edge ($>30 \text{ kHz}$), dn/dt is typically $-5 \times 10^{-4}/\text{cm}^3\text{-s}$. In contrast, for emissions primarily corresponding to the ring-ionosphere density enhancement located near Cassini’s gap ($<30 \text{ kHz}$), dn/dt is typically $+3 \times 10^{-4}/\text{cm}^3\text{-s}$.

3. Plasma Sources and Sinks at the Torus Inner Edge

[16] We define “mass unloading” as any process that removes quasi-corotating plasma from flux tubes in the torus/magneto-disk system. Plasma that is absorbed by the ring particles, by definition, is unloaded from its respective flux tube (to either be neutralized at the ring surface or move on Keplerian orbits attached to the dust) with a mass loss rate defined by L . If we assume that the dn/dt of the active z-mode source regions is representative of the change in quasi-neutral plasma density around the entire annulus

Table 1. An Analysis of the Drift in Specific, Intense Z-Mode Tones^a

	f_{p1} , kHz	t_1 (SCET)	f_{p2} , kHz	t_2 (SCET)	n_1 , cm^{-3}	n_2 , cm^{-3}	dn/dt , $10^{-4} \text{cm}^{-3}\text{s}^{-1}$
Tone 1	58	02:55	58	03:55	41.5	41.5	0
Tone 2	50	02:55	49	04:00	30.8	29.6	-3.0
Tone 3	46.5	02:55	44	03:55	26.7	23.9	-7.8
Tone 4	35	02:55	33	04:00	15.1	13.4	-4.3
Tone 5	17	02:55	19.2	03:35	3.6	4.6	4.0
Tone 6	14.5	03:10	15.5	03:37.5	2.6	3.0	2.1

^aThe start and stop frequency/time is listed, and the corresponding change in density is derived.

that defines the inner torus boundary, then we can express the mass loss as

$$L = 2 m_i z A (dn/dt) \quad (1)$$

where m_i is the dominate ion mass (water from Enceladus), z represents the off-equator dimension of the torus, A is the annulus area, and dn/dt represents the change in plasma density as a function of time as defined by the z-mode tones above 30 kHz (Tones 2–4 in Table 1). The radii defining the annulus is defined by the region where most of the inner torus undergoes its largest density drop, this occurring between 2.0 and 2.3 R_s . This location corresponds to the outer edge of the A-ring and has an area of $\sim 1.3 \times 10^{16} \text{ m}^2$. We initially assume both sides of the rings absorb equally well, leading to the factor of 2 in equation (1). Given $z \sim 4 R_s$ [Richardson and Jurac, 2004; Persoon et al., 2006], then the mass unloading of torus plasma is $L \sim 40 \text{ kg/s}$, which corresponds to about 20–40% of the plasma mass loading occurring near Enceladus [Tokar et al., 2006; Pontius and Hill, 2006].

[17] In our interpretation of the drifting z-mode tones, we explicitly assumed that their sources are part of the inward-diffusing fluid. Hence, the downward drift of the tones is assumed to be indicative of a source density that steadily decreases as the fluid is absorbed at the outer edge of the A-ring. This assumption can be tested by comparing the fluid speed suggested by the z-mode drifts to the actual ion speed. Consider the simple situation where all ion flux is lost when in direct contact with the solid rings (similar to the loss of a lab plasma at any chamber wall). In this case, the mass loss rate is $L \sim 2 m_i n_i v_i A$ where $n_i v_i$ is the particle flux incident on the ring face of area A . We note that this flux loss, $n_i v_i$ should then be comparable to $z dn/dt$ in equation (1) (with dn/dt inferred from the temporal evolution of the z-mode tones). Hence, we can equate these expressions and arrive at an ion velocity consistent with the z-mode tones and the derived dn/dt :

$$v_i \sim (z/n_i) dn/dt \quad (2)$$

For $n_i \sim 30/\text{cm}^3$ and variable z and dn/dt like that used in equation (1), we find that $v_i \sim 4 \text{ km/sec}$ or $\sim 1 \text{ eV}$ for an O^+ -like ion. This value is consistent with O^+ observations made in the inner and middle A-ring [Tokar et al., 2005]. The reasonable value of this speed lends some support to our assumption that the downdrifting z-mode tones are indicative of ion flux loss ($n_i v_i$) at the solid boundary created by the rings.

[18] Consider now the plasma source at the Cassini gap. A model of the ring-ionosphere was presented by Bouhram et al. [2006] that shows O^+ plasma enhancement in the gap. Because the rings are tilted, the ring-ionosphere is asymmetric: there is creation of a sunlit, heavy ionized gas over the south face of the ring and an unlit, weakly ionized gas over the north face of the ring. The rings effectively block plasma transport from south to north side, thereby forming the latitudinally asymmetric ring-ionosphere [Bouhram et al., 2006, Figure 2]. However, plasma is enhanced locally on the nightside face at the Cassini gap from direct transport through the gap. The spacecraft flew over this enhancement at 03:45 SCET and RPWS detected a clear and distinct local increase in plasma frequency (electron density) which is evident in Figure 1.

[19] Note in Figure 1 that a set of z-mode tones below 25 kHz originate near this density enhancement. These tones (e.g., tones 5 and 6 in Table 1) also up-drift in frequency, consistent with a local plasma source at the gap. These tones suggest a density growth, dn/dt , of $\sim 3 \times 10^2/\text{cm}^3\text{-s}$. Assuming this plasma source gets picked up by the magnetic field, the resulting mass loading near the gap is thus

$$S = 2 m_i z A (dn/dt) \quad (3)$$

with m_i being the oxygen mass, $z \sim 0.5 R_s$ [Bouhram et al., 2006], A is the annulus defined by the Cassini gap and dn/dt is derived from the direct observations of the density growth from the z-mode source regions (Table 1). The source of gap ring-ionosphere plasma (on the ring north side) is then $S \sim 1\text{--}2 \text{ kg/s}$.

[20] We note that the ring-ionosphere plasma source associated with the Cassini gap is a spatially-isolated source that merges seamlessly with the torus loss region in the middle of the A ring. Because of radial diffusion, the ring-ionosphere plasma diffuses outward and torus plasma continues to diffuse inward, respectively, and interact on

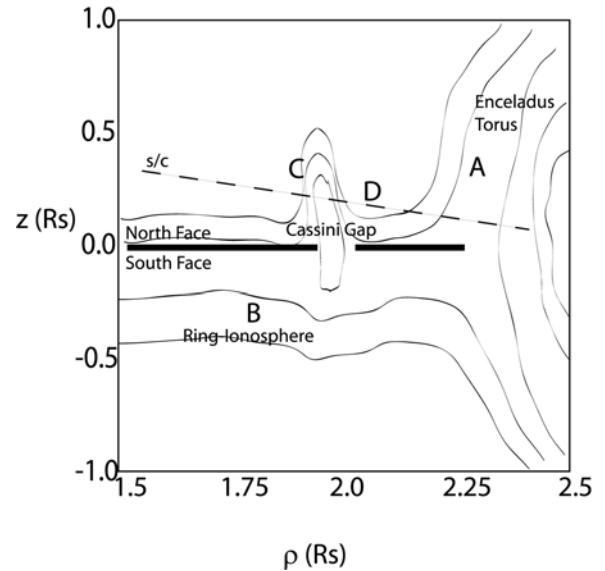


Figure 3. An illustration of the plasma morphology at the ring/torus region. Regions of interest are labeled and discussed further in section 4.

common field lines in the central A ring. We note in Figure 1 that there is a relative minima in plasma density at 03:52 SCET, near $2.02 R_s$. Jurac and Richardson [2007] recently suggested that the outer rings may show a brightening due to Enceladus-originating water deposition. We herein provide further evidence of this Enceladus/outer-ring mass exchange via the clear signature of plasma torus absorption at the rings.

4. Conclusions

[21] We demonstrate that the inner edge of the Enceladus plasma torus is indeed a very complicated ring/plasma interface. In examining plasma density profiles alone, it is relatively difficult to determine where the Enceladus torus ends and the ring-ionosphere plasma dominates. Fortunately, this inner edge is active and radiates remotely-propagating z-mode from active regions with intensified f_p emission [Farrell et al., 2005]. The emission, in essence, “tags” the active plasma sources at various locations and allows a method to remote-sense the source plasma evolution. By monitoring the temporal evolution of the z-mode tones, we are able to infer dn/dt and hence regions of source and losses. The inference implicitly assumes that the z-mode tones are directly indicative of the plasma fluid density evolution in the A-ring absorbing region. While this assumption is not unique (other possible ways to interpret the drifting in z-mode tones), the evolution of the tone-derived density change with time (dn/dt) is consistent with the loss of water-like ion flux directly onto the ring (see equation 2), bolstering the assumption.

[22] Figure 3 illustrates the morphology of the plasma at the Enceladus torus/ring interface region. In region A, Enceladus torus plasma is absorbed at the outer A-ring at a rate of ~ 40 kg/s, as inferred from the z-mode downdrifting tones. In region B, there is a substantial ring-ionosphere on the south sun-facing ring surface as modeled by Bouhram et al. [2006]. On the north face, this ring-ionosphere plasma is vastly reduced except at the Cassini gap (region C), where transport will create a source at $1-2$ kg/s (as inferred from the z-mode updrifting tones originating from the region). There is a distinct minimum in plasma in the middle of the A-ring (region D) where low density Enceladus torus and ring-ionosphere plasma appear to merge and coincide; this minimum evident in local f_p at 03:52 SCET near $2.02 R_s$.

[23] **Acknowledgments.** We gratefully thank the Cassini science project at JPL and HQ which funds this research. The research at the University of Iowa is supported by NASA through contract 1279973 via JPL. We also thank the data processing team at the PI institution at the University of Iowa who have developed a great set of tools for a Co-I team that is spread across continents.

References

Bouhram, M., R. E. Johnson, J.-J. Berthelier, J.-M. Illiano, R. L. Tokar, D. T. Young, and F. J. Cray (2006), A test-particle model of the atmosphere/

- ionosphere system of Saturn's main rings, *Geophys. Res. Lett.*, *33*, L05106, doi:10.1029/2005GL025011.
- Farrell, W. M., W. S. Kurth, M. L. Kaiser, M. D. Desch, D. A. Gurnett, and P. Canu (2005), Narrowband Z-mode emissions interior to Saturn's plasma torus, *J. Geophys. Res.*, *110*, A10204, doi:10.1029/2005JA011102.
- Gurnett, D. A., et al. (2004), The Cassini radio and plasma wave investigation, *Space Sci. Rev.*, *114*.
- Gurnett, D. A., et al. (2005), Cassini radio and plasma wave observations near Saturn, *Science*, *307*, 1255.
- Gurnett, D. A., et al. (2007), The variable rotation period of the inner region of Saturn's plasma disk, *Science*, *316*, 442.
- Hansen, C. J., et al. (2006), Enceladus' water vapor plume, *Science*, *311*, 1422.
- Johnson, R. E., et al. (2006), The Enceladus and OH Tori at Saturn, *Astrophys. J.*, *644*, L137.
- Jurac, S., and J. D. Richardson (2005), A self-consistent model of plasma and neutrals at Saturn: Neutral cloud morphology, *J. Geophys. Res.*, *110*, A09220, doi:10.1029/2004JA010635.
- Jurac, S., and J. D. Richardson (2007), Neutral cloud interaction with Saturn's main rings, *Geophys. Res. Lett.*, *34*, L08102, doi:10.1029/2007GL029567.
- Jurac, S., et al. (2002), Saturn: Search for a missing water source, *Geophys. Res. Lett.*, *29*(24), 2172, doi:10.1029/2002GL015855.
- Persoon, A. M., D. A. Gurnett, W. S. Kurth, G. B. Hospodarsky, J. B. Groene, P. Canu, and M. K. Dougherty (2005), Equatorial electron density measurements in Saturn's inner magnetosphere, *Geophys. Res. Lett.*, *32*, L23105, doi:10.1029/2005GL024294.
- Persoon, A. M., D. A. Gurnett, W. S. Kurth, and J. B. Groene (2006), A simple scale height model of the electron density in Saturn's plasma disk, *Geophys. Res. Lett.*, *33*, L18106, doi:10.1029/2006GL027090.
- Pontius, D. H., and T. W. Hill (2006), Enceladus: A significant plasma source for Saturn's magnetosphere, *J. Geophys. Res.*, *111*, A09214, doi:10.1029/2006JA011674.
- Porco, C. C., et al. (2006), Cassini observes the active south pole of Enceladus, *Science*, *311*, 1393.
- Richardson, J. D., and S. Jurac (2004), A self-consistent model of plasma and neutrals at Saturn: The ion tori, *Geophys. Res. Lett.*, *31*, L24803, doi:10.1029/2004GL020959.
- Richardson, J. D., A. Eviatar, M. A. McGrath, and V. M. Vasyliunas (1998), OH in Saturn's magnetosphere: Observations and implications, *J. Geophys. Res.*, *103*, 20,245.
- Shemansky, D. E., et al. (1993), Detection of the hydroxyl radical in Saturn's magnetosphere, *Nature*, *363*, 329.
- Tokar, R. L., et al. (2005), Cassini observations of the thermal plasma in the vicinity of Saturn's main rings and the F and G rings, *Geophys. Res. Lett.*, *32*, L14S04, doi:10.1029/2005GL022690.
- Tokar, R. L., et al. (2006), The interaction of the atmosphere of Enceladus with Saturn's plasma, *Science*, *311*, 1409.
- Van Allen, J. A., et al. (1980), Saturn's magnetosphere, rings, and inner satellites, *Science*, *207*, 415.
- Wahlund, J.-E., et al. (2005), The inner magnetosphere of Saturn: Cassini RPWS cold plasma results from the first encounter, *Geophys. Res. Lett.*, *32*, L20S09, doi:10.1029/2005GL022699.
- Waite, J. H., Jr., et al. (2006), Cassini ion and neutral mass spectrometer: Enceladus plume composition and structure, *Science*, *311*, 1419.
- Xin, L., D. A. Gurnett, and M. G. Kivelson (2006), Whistler mode auroral hiss emissions observed near Jupiter's moon Io, *J. Geophys. Res.*, *111*, A04212, doi:10.1029/2005JA011411.

P. Canu, CETP, 10-12 Avenue de l'Europe, F-78140 Velizy, France.
 W. M. Farrell and M. L. Kaiser, NASA/Goddard SFC, Greenbelt, MD 20771, USA. (william.farrell@gssc.nasa.gov)
 D. A. Gurnett, W. S. Kurth, and A. M. Persoon, Department of Physics and Astronomy, University of Iowa, Iowa City, IA 52240, USA.
 J. E. Wahlund, Swedish Institute of Space Physics, SE-751 21 Uppsala, Sweden.